

SUPERLUMINOUS SUPERNOVA IPTF13EHE: FIRST EVIDENCE OF TRIPLE ENERGY SOURCES

S. Q. WANG^{1,2}, L. D. LIU^{1,2}, Z. G. DAI^{1,2}, L. J. WANG³, AND X. F. WU^{4,5,6}

¹School of Astronomy and Space Science, Nanjing University, Nanjing 210093, China; dzg@nju.edu.cn

²Key Laboratory of Modern Astronomy and Astrophysics (Nanjing University), Ministry of Education, China

³Key Laboratory of Space Astronomy and Technology, National Astronomical Observatories, Chinese Academy of Sciences, Beijing 100012, China

⁴Purple Mountain Observatory, Chinese Academy of Sciences, Nanjing, 210008, China

⁵Chinese Center for Antarctic Astronomy, Chinese Academy of Sciences, Nanjing, 210008, China and

⁶Joint Center for Particle Nuclear Physics and Cosmology of Purple Mountain Observatory-Nanjing University, Chinese Academy of Sciences, Nanjing 210008, China

Draft version October 10, 2018

ABSTRACT

Almost all superluminous supernovae (SLSNe) whose peak magnitudes are $\lesssim -21$ mag can be explained by the ^{56}Ni -powered model or magnetar-powered (highly magnetized pulsar) model or ejecta-circumstellar medium (CSM) interaction model. Recently, iPTF13ehe challenges these energy-source models, because the spectral analysis indicates that $\sim 2.5M_{\odot}$ of ^{56}Ni have been synthesized but are inadequate to power the peak bolometric emission of iPTF13ehe, while the rebrightening of the late-time light-curve (LC) and the $\text{H}\alpha$ emission lines indicate that the ejecta-CSM interaction must play a key role in powering the late-time LC. In this *Letter*, we show that the early LC of iPTF13ehe can be powered by a magnetar together with a large amount of ^{56}Ni , while the late-time LC may be attributed to all three energy sources listed above. Therefore, iPTF13ehe is the first SLSN powered by triple energy sources. Furthermore, we propose that iPTF13ehe is a genuine core-collapse supernova (CCSN) rather than a pulsational pair-instability supernova (PPISN) candidate. Further studies on similar SLSNe in the future would eventually shed light on the nature of the explosion mechanisms and energy-mechanisms of these SLSNe.

Subject headings: stars: magnetars – supernovae: general – supernovae: individual (iPTF13ehe)

1. INTRODUCTION

Supernovae (SNe) are exceptionally brilliant stellar explosions in the Universe. Over the last decade, dozens of superluminous SNe (SLSNe) whose peak magnitudes are $\lesssim -21$ mag (Gal-Yam 2012) have attracted intense interest from both observational and theoretical astronomers. SLSNe are the rarest class of supernovae discovered so far and have been classified into types I (hydrogen-poor) and II (hydrogen-rich). The ratio of the explosion rates of SLSNe to core-collapse SNe (CCSNe) is $\sim 10^{-4}$ (e.g. Gal-Yam 2012).

Discriminating among the energy-sources powering the SLSNe is rather tricky. However, these energy sources should leave their imprints on the light curves (LCs) and the spectra of these SLSNe. Only very few SLSNe can be regarded as the so-called “pair instability SNe (PISNe)” (Barkat et al. 1967; Rakavy & Shaviv 1967; Heger & Woosley 2002; Heger et al. 2003) and explained by the ^{56}Ni -powered model (Gal-Yam et al. 2009), while the majority of SLSNe cannot be powered purely by ^{56}Ni (Quimby et al. 2011; Inserra et al. 2013) and can be explained by the ejecta-circumstellar medium (CSM) interaction model (Chevalier & Irwin 2011; Ginzburg & Balberg 2012) or magnetar-powered (ultra-highly magnetized pulsar) model (Kasen & Bildsten 2010; Woosley 2010; Dessart et al. 2012; Inserra et al. 2013; Wang et al. 2015a). Due to the absence of emission lines indicative of the ejecta-CSM interaction, the magnetar model is preferred in explaining almost all SLSNe I (e.g. Inserra et al. 2013; Nicholl et al. 2013; Howell et al. 2013; McCrum et al. 2014; Vreeswijk et al.

2014; Nicholl et al. 2014; Wang et al. 2015a; Kasen et al. 2015; Metzger et al. 2015; Dai et al. 2015). Meanwhile, the ejecta-CSM interaction model works well in explaining SLSNe II, especially superluminous SNe IIn (Smith & McCray 2007; Moriya et al. 2013a).

In principle, ^{56}Ni should be taken into account in light-curve modeling for all SLSNe. From the photometric aspect, however, SLSNe’s ^{56}Ni yields are usually rather small and the luminosities provided by ^{56}Ni are outshone by magnetars or ejecta-CSM interaction. Besides, ^{56}Ni yields can be inferred via the late-time nebular spectral analysis and are difficult to be determined precisely owing to the lack of late-time spectra for most SNe. Hence, excluding a few pair-instability supernova (PISN) candidates, previous modelings for most LCs of SLSNe I omitted the contributions of ^{56}Ni . There are some more complicated cases: for some SLSNe II, e.g. SN 2006gy, adding several M_{\odot} of ^{56}Ni can make the fitting more reliable, the “ ^{56}Ni +interaction” model has been employed (Agnoletto et al. 2009; Chatzopoulos et al. 2012, 2013). No SLSN has involved with all three energy sources so far.

Recently, an SLSN I at redshift $z = 0.3434$, iPTF13ehe, might change the conclusions above. Yan et al. (2015) analyzed the light curve and spectra of iPTF13ehe and found that the peak bolometric luminosity of iPTF13ehe is $\sim 1.3 \times 10^{44}$ erg s^{-1} . If this SLSN was powered by ^{56}Ni , more than $13 - 16M_{\odot}$ of ^{56}Ni must be synthesized to power the peak bolometric emission (Yan et al. 2015). However, the late-time spectral analysis indicated that the mass of ^{56}Ni produced by

the SLSN is $\sim 2.5 M_{\odot}$. This amount of ^{56}Ni , although cannot be ignored, is inadequate to power the peak bolometric luminosity. Therefore, Yan et al. (2015) argued that the early LC must be powered by multiple power sources.

Furthermore, the presence of H α emission lines in the late-time spectrum and the rebrightening in the late-time LC show an unambiguous signature for interactions between the SN ejecta and a hydrogen-rich CSM. Hence, any model with single power source or double power sources is challenged in explaining the LC of iPTF13ehe. A triple-power-source model should be seriously considered.

Here we investigate the energy sources of iPTF13ehe and try to understand its explosion mechanism. This Letter is organized as follows. In Sections 2 and 3, we fit the early-time and late-time LC using double and triple energy-source models, respectively. In Section 4, we discuss and conclude our results.

2. MODELING THE EARLY-TIME LC

We start by studying the early LC and determining the power sources of iPTF13ehe. As pointed out by Yan et al. (2015), $\sim 2.5 M_{\odot}$ of ^{56}Ni were synthesized while $\gtrsim 13 - 16 M_{\odot}$ of ^{56}Ni are required to account for the LC peak. Therefore, there should be other energy sources to aid the high peak-luminosity of iPTF13ehe. The early-time spectra shows no H emission lines, indicating that the ejecta-CSM interaction can be neglected in the early-time luminosity evolution. Hence, the energy source aiding the SN might be a magnetar spin-down input. Considering the contribution from ^{56}Ni which cannot be neglected, the most reasonable model is the one that contains contributions from both ^{56}Ni and a magnetar. Wang et al. (2015b) have constructed such a unified model for SNe Ic and explained three luminous SNe Ic. We here employ this model to fit the LC of iPTF13ehe.

Supposing that the ratio of the r -band flux to bolometric flux remains nearly constant around the peak and in the late-time, we scale the r -band luminosities to obtain the bolometric luminosities. The scaled bolometric luminosities are rough, but they can be regarded as rough approximations of real values. These data are plotted in Fig. 1.

The photospheric velocity is fixed to $\sim 13,000 \text{ km s}^{-1}$ (Yan et al. 2015). We find that when the ejecta mass $M_{\text{ej}} = 35 M_{\odot}$, the ^{56}Ni mass $M_{\text{Ni}} = 2.5 M_{\odot}$, the optical opacity $\kappa = 0.2 \text{ cm}^2 \text{ g}^{-1}$, the gamma-ray opacity $\kappa \simeq 0.018 \text{ cm}^2 \text{ g}^{-1}$, the initial rotational period of the magnetar $P_0 = 2.55 \text{ ms}$, the surface magnetic field $B = 8 \times 10^{13} \text{ G}$, the theoretical LC can match the observational data at early times ($t \lesssim 137 \text{ days}$), as can be seen in Fig. 1.

If we ignore the contribution from ^{56}Ni , to obtain an equivalently well fitting, the initial period of the magnetar P_0 has to be lowered slightly, $P_0 \sim 2.45 \text{ ms}$. When the contribution from the magnetar is neglected, the ^{56}Ni mass M_{Ni} should be $\sim 19 M_{\odot}$, slightly larger than the value ($\sim 13 - 16 M_{\odot}$) inferred by Yan et al. (2015). Both models are unreasonable since the spectral analysis has demonstrated that the SN explosion produced $\sim 2.5 M_{\odot}$ of ^{56}Ni . Therefore, the model containing the contributions from ^{56}Ni and a magnetar is the most reasonable one accounting for the early-time LC of iPTF13ehe.

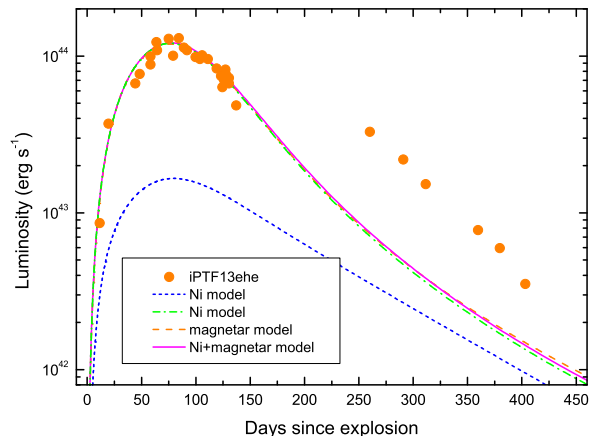


FIG. 1.— Modeling iPTF13ehe’s early-time LC using the unified model (^{56}Ni , magnetar, and hybrid ($^{56}\text{Ni} + \text{magnetar}$)). Data are obtained from Yan et al. (2015). The bolometric luminosities scaled from r -band ones are shown as the orange filled circles. The dash-dotted line is the LC powered by $19 M_{\odot}$ of ^{56}Ni ; the dashed line is the LC powered by a magnetar; the solid line is the LC powered by ^{56}Ni and a magnetar. The short dashed line is the LC powered by $2.5 M_{\odot}$ of ^{56}Ni with full trapping of gamma-rays. The other model parameter values are shown in the context.

A caveat on the degeneracy of model parameters should be clarified here. The effective light-curve timescale $\tau_m = (2\kappa M_{\text{ej}}/\xi v c)^{1/2}$ (Arnett 1982) determines the width and therefore the rise time of the LCs of SNe, where c is the speed of light and $\xi = 4\pi^3/9 \simeq 13.8$ is a constant. If the value of $\kappa M_{\text{ej}}/v$ is invariant, LCs around the peak are same. Although the photospheric velocity v of iPTF13ehe is fixed to $13,000 \text{ km s}^{-1}$, the degeneracy of κ and M_{ej} is still difficult to be broken, because larger κ requires smaller M_{ej} for the same level of fittings. The optical opacity of H- and He-deficient ejecta is rather uncertain, its value has been assumed to be $0.06 \text{ cm}^2 \text{ g}^{-1}$ (e.g., Valenti et al. 2011; Lyman et al. 2014), $0.07 \text{ cm}^2 \text{ g}^{-1}$ (e.g., Taddia et al. 2015; Wang et al. 2015b), $0.08 \text{ cm}^2 \text{ g}^{-1}$ (e.g., Arnett 1982; Mazzali et al. 2000), $0.10 \text{ cm}^2 \text{ g}^{-1}$ (e.g., Nugent et al. 2011; Inserra et al. 2013; Wheeler et al. 2015), and $0.2 \text{ cm}^2 \text{ g}^{-1}$ (e.g., Kasen & Bildsten 2010; Nicholl et al. 2014). We assume that $\kappa = 0.2 \text{ cm}^2 \text{ g}^{-1}$ throughout this Letter and get the ejecta mass $M_{\text{ej}} \sim 35 M_{\odot}$. If we assume a smaller κ , e.g., $\kappa = 0.1 \text{ cm}^2 \text{ g}^{-1}$, then the ejecta mass is very large, $M_{\text{ej}} \sim 70 M_{\odot}$. The latter is consistent with the lower limit derived by Yan et al. (2015). Provided that iPTF13ehe is a genuine core-collapse SN, an ejecta with mass of $35 M_{\odot}$ is preferred.

From the fit, we can get two other important physical quantities relevant to the next section, i.e., the rise time $t_r \sim 81 \text{ days}$ and the kinetic energy of the SN explosion, $E_{\text{SN}} = (3/10)M_{\text{ej}}v^2 \sim 3.5 \times 10^{52} \text{ erg}$.

3. MODELING THE LATE-TIME LC

We have demonstrated that the hybrid model containing the contributions from ^{56}Ni and a magnetar can well fit the early-time LC of iPTF13ehe, but the late-time rebrightening cannot be explained by such a hybrid model.

Yan et al. (2015) found that the late-time spectrum of the SN displayed H α emission lines which are usually present in SNe IIn and inferred that a Hydrogen shell ejected about 40 years before the SN explosion, locating at a distance of $\sim 4 \times 10^{16}$ cm from the SN progenitor. When the SN ejecta run into the shell, an interaction was triggered, then the r -band LC was rebrightened and the H α emission was prompted. Therefore, both the photometric and spectral features indicate that the interaction between the ejecta and CSM must play an important role in powering the late-time LC.

However, the exact time of the emergence of the ejecta-CSM interaction is uncertain due to the lack of the photometric data at $\sim 60 - 170$ days and the spectral data at 13 – 251 days after the peak. Nevertheless, the fact that there is no rebrightening before ~ 56 days after the peak provides a lower limit on the interaction onset time, while the rebrightening at ~ 180 days after the peak offers an upper limit. Therefore, we suppose that the rebrightening started at $\sim 56 - 180$ days after the peak. Adopting $t_r \sim 81$ days, we conclude that the interaction should be triggered between $\sim 137 - 261$ days after the SN explosion. Hence, $t_i = 140$ days is reasonable.

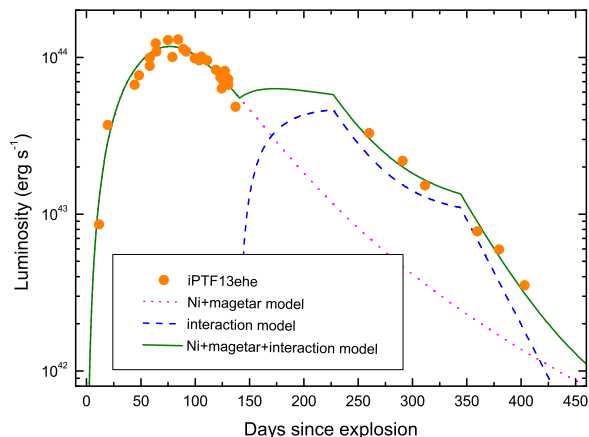


FIG. 2.— Modeling iPTF13ehe’s whole LC using the grand unified model (^{56}Ni + magnetar + interaction). Data are obtained from Yan et al. (2015). The bolometric luminosities scaled from r -band ones are shown as the orange filled circles. The dotted line is the LC powered by ^{56}Ni and a magnetar; the dashed line is the LC powered by the ejecta-CSM interaction; the solid line is the LC powered by the triple energy source (^{56}Ni +magnetar+ejecta-CSM interaction”) model. The other model parameter values are shown in the context.

According to Equations (14)-(16) and (20) of Chatzopoulos et al. (2012), we reproduce the late-time LC powered by the ejecta-CSM interaction, seen in Fig. 2. The fit parameters are: the optical opacity of the H-shell $\kappa' = 0.34 \text{ cm}^2 \text{ g}^{-1}$, the ejecta mass $M_{\text{ej}} = 35M_{\odot}$, the SN kinetic energy $E_{\text{SN}} = 3.5 \times 10^{52}$ erg (these two parameters are derived from the previous section), the slope of the inner density profile of the ejecta $\delta = 0$, the slope of the outer density profile of the ejecta $n = 7$, the power-law exponent for the CSM density profile $s = 0$ (corresponding to a uniform-density shell), the density

of the CSM $\rho_{\text{CSM}} = 10^{-14} \text{ g cm}^{-3}$, the mass of the CSM $M_{\text{CSM}} = 27M_{\odot}$, the onset time of interaction between the ejecta and the CSM-shell t_i is ~ 140 days, the conversion efficiency from kinetic energy to radiation $\epsilon = 0.05$ which is comparable to the typical value $\epsilon \sim 0.1$ (Moriya et al. 2013b).

The density of the CSM shell in our model is one order of magnitude larger than the value derived by Yan et al. (2015). Since the shock-ionized CSM shell is probably optically thin to the Thomson scattering (Yan et al. 2015), $\tau_{\text{Thomson}} = \kappa' \rho w \leq 1$, where w is the width of the shell, then $\kappa' (M_{\text{CSM}}/4\pi R^2 w) w = \kappa' (M_{\text{CSM}}/4\pi R^2) \leq 1$, so $M_{\text{CSM}} \leq 4\pi R^2/\kappa'$. Yan et al. (2015) supposed that the interaction time is 251 days after the peak, and derived that $R \simeq 4 \times 10^{16}$ cm. If $w = 0.1R$, and $\kappa' = 0.34 \text{ cm}^2 \text{ g}^{-1}$, then $M_{\text{CSM}} \leq 30M_{\odot}$, $n = \rho/m_{\text{H}} \leq 1/\kappa' w m_{\text{H}} \sim 4 \times 10^8 \text{ cm}^{-3}$ (Yan et al. 2015), and $\rho \leq 0.74 \times 10^{-15} \text{ g cm}^{-3}$.

This difference is partly caused by the uncertainty of the onset time of the ejecta-CSM interaction. We suppose that the interaction time is ~ 60 days after the peak, then $R = vt \sim 1.6 \times 10^{16}$ cm; if $w = 0.1R$, and $\kappa' = 0.34 \text{ cm}^2 \text{ g}^{-1}$, then $M_{\text{CSM}} \leq 5M_{\odot}$, $n \leq 1.1 \times 10^9 \text{ cm}^{-3}$, and $\rho \leq 1.84 \times 10^{-15} \text{ g cm}^{-3}$. As pointed out by Yan et al. (2015), the possibility that the CSM shell might be partly ionized rather than fully ionized cannot be excluded. Provided that the ratio of ionized CSM to total CSM is $\sim 1/5.4$, then $\rho_{\text{CSM}} \sim 10^{-14} \text{ g cm}^{-3}$, and $M_{\text{CSM}} \sim 27M_{\odot}$, being consistent with the values of our fitting parameters.

As shown in Fig. 2, the LC powered by the triple power-source model (“ ^{56}Ni +magnetar+ejecta-CSM interaction” model) is well consistent with the data. We call the extended unified model as the “grand unified model” which contains all three types of power sources explaining SLSNe.

4. DISCUSSION AND CONCLUSIONS

We have analyzed and fitted the LC for iPTF13ehe which is an SLSN I with peak bolometric luminosity $\sim 1.3 \times 10^{44} \text{ erg s}^{-1}$.

Spectral analysis performed by Yan et al. (2015) shows that the SLSN synthesized $\sim 2.5M_{\odot}$ of ^{56}Ni and this amount of ^{56}Ni is inadequate to power the peak. We proposed that the most reasonable model accounting for the early-time LC is the hybrid model containing the contributions from a magnetar with $P_0 = 2.55$ ms and $B = 8 \times 10^{13}$ G and $2.5M_{\odot}$ of ^{56}Ni . The LC reproduced by the hybrid model is in good agreement with early-time observations for iPTF13ehe. The energy released by the magnetar is still dominant in powering the optical LC of iPTF13ehe. We also fitted the LC using the magnetar model without any ^{56}Ni . In the pure magnetar model, initial period the magnetar is ~ 2.45 ms, slightly lower than the value adopted in the hybrid model. Neglecting the contribution from the magnetar, we found that $\sim 19M_{\odot}$ of ^{56}Ni are required, confirming the conclusion reached by Yan et al. (2015).

Wang et al. (2015b) emphasized that this unified scenario is especially important for some luminous SNe Ic with peak magnitudes ~ -20 mag since they cannot be powered solely by ^{56}Ni (see also Greiner et al. 2015) but the contribution from ^{56}Ni cannot be neglected. Here, we

find that when the ^{56}Ni yield is large enough, it should also be considered in the modelings, although lowering slightly the initial period of the magnetar can compensate for the contribution from ^{56}Ni .

Another important spectral feature owned by iPTF13ehe is $\text{H}\alpha$ emission lines in its late-time spectrum. The $\text{H}\alpha$ emission lines, together with the rebrightening of the late-time LC, indicate that the interaction between the SN ejecta and the CSM has been triggered. The hybrid model involving ^{56}Ni and magnetar cannot account for the late-time rebrightening. We find that the ejecta-CMS interaction model can explain the rebrightening and is the natural requirement accounting for the $\text{H}\alpha$ emission lines. Therefore, we use the “grand unified model” which contains all three energy sources (^{56}Ni , magnetar and ejecta-CMS interaction) and fit the whole LC.

In summary, we have shown that the early-time LC of iPTF13ehe should be powered by two energy sources (^{56}Ni and magnetar) while the late-time LC must be explained by the triple energy-source model. Therefore, iPTF13ehe may be the first SLSN requiring triple energy sources.

We caution that the bolometric LC is obtained by scaling the r -band LC and therefore is not accurate enough. The uncertainties in the bolometric luminosities prevent us from getting precise estimate of the model parameters. Nevertheless, this does not change the facts that the early-time LC needs double energy sources and that the late-time LC requires triple energy sources. More accurate bolometric corrections can pose more stringent constraints on the parameters.

Finally, we discuss the nature of the explosion of iPTF13ehe. The physical properties of the progenitors, the explosion mechanisms and energy-source mechanisms of SLSNe are still ambiguous and in debate (see

Dessart et al. 2012; Nicholl et al. 2013, for further analysis). As emphasized by Yan et al. (2015), the massive Hydrogen-rich shell must have been expelled by the “pulsational pair-instability (PPI)” mechanism (Heger et al. 2003; Woosley et al. 2007; Pastorello et al. 2008; Chugai 2009; Chatzopoulos & Wheeler 2012). The ejecta colliding with CSM shell contains $\sim 2.5M_{\odot}$ of ^{56}Ni and $\gtrsim 3.5 \times 10^{52}$ erg of kinetic energy. This ejecta is not a shell following the hydrogen-rich shell, because Heger et al. (2003) pointed out that the shell expelled by PPI contains no ^{56}Ni and its kinetic energy is up to several times 10^{51} erg. The kinetic energy of the ejecta of iPTF13ehe is at least one order of magnitude higher than the value of each PPI pulsed shell. The ^{56}Ni yield ($2.5M_{\odot}$) is also inconsistent with the zero ^{56}Ni mass predicted by the PPI mechanism. Therefore, we propose that iPTF13ehe itself is a genuine CCSN rather than a PPISN candidate, while the hydrogen-rich massive shell could be caused by a PPI pulse ~ 20 years before the CCSN explosion ($\delta t \sim vt_i/v_{\text{CSM}} \sim 13,000 \text{ km/s} \times 140 \text{ days}/300 \text{ km/s} \sim 17$ years, the value of velocity of the CSM shell v_{CSM} was inferred by Yan et al. (2015)).

We expect that future studies focusing on similar SLSNe should provide further insight into the explosion mechanisms and energy-mechanisms of these SLSNe.

This work was supported by the National Basic Research Program (973 Program) of China (grant No. 2014CB845800) and the National Natural Science Foundation of China (grant Nos. 11573014 and 11322328). X.F.W. is partially supported by the One-hundred-talents Program, the Youth Innovation Promotion Association (2011231), and the Strategic Priority Research Program The Emergence of Cosmological Structures (grant No. XDB09000000) of the Chinese Academy of Sciences.

REFERENCES

- Agnoletto I, Benetti S, Cappellaro E, et al. ApJ, 2009, 691, 1348
 Arnett, W. D. 1982, ApJ, 253, 785
 Barkat, Z., Rakavy, G., & Sack, N. 1967, Phys. Rev. Lett., 18, 379
 Chatzopoulos, E., & Wheeler, J. C. 2012, ApJ, 760, 154
 Chatzopoulos, E., Wheeler, J. C., & Vinko, J. 2012, ApJ, 746, 121
 Chatzopoulos, E., Wheeler, J. C., Vinko, J., Horvath, Z. L., & Nagy, A. 2013, ApJ, 773, 76
 Chevalier, R. A., & Irwin, C. M. 2011, ApJL, 729, L6
 Chugai, N. N. 2009, MNRAS, 400, 866
 Dai, Z. G., Wang, S. Q., Wang, J. S., Wang, L. J., & Yu, Y. W. 2015, submitted, arXiv:1508.07745
 Dessart, L., Hillier, D. J., Waldman, R., Livne, E., & Blondin, S. 2012, MNRAS, 426, L76
 Gal-Yam, A., Mazzali, P., Ofek, E. O., et al. 2009, Nature, 462, 624
 Gal-Yam, A. 2012, Science, 337, 927
 Ginzburg, S., & Balberg, S. 2012, ApJ, 757, 178
 Greiner, J., Mazzali, P. A., Kann, D. A., et al. 2015, Nature, 523, 189
 Heger, A., & Woosley, S. E. 2002, ApJ, 567, 532
 Heger, A., Fryer, C. L., Woosley, S. E., Langer, N. & Hartmann, D. H. 2003, ApJ, 591, 288
 Howell, D. A., Kasen, D., Lidman, C., et al. 2013, ApJ, 779, 98
 Inserra, C., Smartt, S. J., Jerkstrand, A., et al. 2013, ApJ, 770, 128
 Kasen, D., & Bildsten, L. 2010, ApJ, 717, 245
 Kasen, D., Metzger, B. D., & Bildsten, L. 2015, submitted to ApJ, arXiv:150703645
 Lyman, J. D., Bersier, D., James, P. A., Mazzali, P. A., Eldridge, J., Fraser, M., & Pian, E. 2014, arXiv:1406.3667
 Mazzali, P. A., Iwamoto, K., & Nomoto, K. 2000, ApJ, 545, 407
 McCrum, M., Smartt, S. J., Kotak, R., et al. 2014, MNRAS, 437, 656
 Metzger, B. D., Margalit, B., Kasen, D., & Quataert, E. 2015, submitted to MNRAS Letters, 2015, arXiv: 1508.02712
 Moriya, T. J., Blinnikov, S. I., Tominaga, N., Yoshida, N., Tanaka, M., Maeda, K., & Nomoto, K. 2013a, MNRAS, 428, 1020
 Moriya, T. J., Maeda, K., Taddia, F., Sollerman, J., Blinnikov, S. I., & Sorokina, E. I. 2013b, MNRAS, 435, 1520
 Nicholl, M., Smartt, S. J., Jerkstrand, A., et al. 2013, Nature, 502, 346
 Nicholl, M., Jerkstrand, A., Inserra, C., et al. 2014, MNRAS, 444, 2096
 Nugent, P. E., Sullivan, M., Cenko, S. B., et al. 2011, Nature, 480, 344
 Pastorello, A., Mattila, S., Zampieri, L., et al. 2008, MNRAS, 389, 113
 Quimby, R. M., Kulkarni, S. R., Kasliwal, M. M., et al. 2011, Nature, 474, 487
 Rakavy, G., & Shaviv, G. 1967, ApJ, 148, 803
 Smith, N., & McCray, R. 2007, ApJL, 671, L17
 Taddia, F., Sollerman, J., Leloudas, G., Stritzinger, M. D., Valenti, S., Galbany, L., Kessler, R., Schneider, D. P., & Wheeler, J. C. 2015, A&A, 574, 60
 Valenti, S., Fraser, M., Benetti, S., et al. 2011, MNRAS, 416, 3138
 Vreeswijk, P. M., Savaglio, S., Gal-Yam, A., et al. 2014, ApJ, 797, 24
 Wang, S. Q., Wang, L. J., Dai, Z. G., & Wu, X. F. 2015a, ApJ, 799, 107

Wang, S. Q., Wang, L. J., Dai, Z. G., & Wu, X. F. 2015b, *ApJ*, 807, 147
Wheeler, J. C., Johnson, V., & Clocchiatti, A. 2015, *MNRAS*, 450, 1295

Woosley, S. E. 2010, *ApJL*, 719, L204
Woosley, S. E., Blinnikov, S., & Heger, A. 2007, *Nature*, 450, 390
Yan, L., Quimby, R., Ofek, E., et al. 2015, submitetd to *ApJ*,
arXiv:1508.04420